JOURNAL OF AIRCRAFT
Vol. 41, No. 2, March–April 2004

Correlations to Predict the Streamwise Influence Regions in Supersonic Turbulent Flows

Manohari D. Ramesh* and John C. Tannehill†
Iowa State University, Ames, Iowa 50011

Correlation functions that can accurately predict the extent of the streamwise regions of influence for two-dimensional supersonic turbulent flows over compression ramps, expansion corners, and shock-impingement flowfields have been developed. These empirically developed correlations that involve known flow parameters can be used to determine the lengths of the streamwise (upstream and downstream) regions of influence. The correlations were obtained by analyzing numerically generated compression ramp, expansion corner, and shock-impingement flowfields. These flowfields were computed using an iterative parabolized Navier–Stokes algorithm in conjunction with the relaxation eddy-viscosity turbulence model of Shang and Hankey. Regression analysis using the least-squares approach was applied to the numerically generated data to determine the correlation functions. The accuracy of the developed correlations is demonstrated by comparing them with experimental and numerical data, and they were found to be accurate in predicting the extent of both the upstream and downstream influence regions.

Introduction

THE problems caused by the presence of shock and expansion waves in two-dimensional supersonic flows are numerous. These problems are compounded in turbulent flows, as turbulence adds to the complexity of the flow. The presence of shock/expansion waves in the flowfield surrounding an aircraft can lead to unacceptably high levels of drag and local heating. These waves result from a change in geometry (such as a compression ramp or an expansion corner) or from an externally generated shock impinging on the aircraft's body. The design of a supersonic vehicle under these conditions would be greatly facilitated if information about the extent of the streamwise interaction region is known a priori.

In the present study correlation functions that can predict the extent of the streamwise regions of influence in a turbulent flow are sought. The influence can be caused either by a change in body geometry, such as the presence of compression ramps or expansion corners, or by a shock impinging on a turbulent boundary layer. To be able to predict the extent of these influence regions, the functions should depend only on known flow variables. Correlations have been developed previously for laminar flows, by Miller et al.,[1] for flow situations involving shock impingement on a flat plate and flow past compression ramps and expansion corners.

Several attempts have been made to correlate the influence region in a two-dimensional turbulent flow over a compression ramp. Numerous experiments have also been conducted for a wide variety of compression ramp flowfields, for example, Refs. 2–11. Settles et al. and colleagues[12,13] have performed the most notable work in correlating the upstream influence region in the presence of a compression ramp, based on the upstream pressure influence criterion. These investigators dealt with the relationship between the upstream influence length and the Reynolds number and/or the angle of the compression ramp, but did not address the effects of the variation of Mach number. The correlation developed by Roshko and Thomke[9] requires the determination of the skin-friction coefficient prior to computing the downstream influence length. These limitations rule out the use of these relations for the a priori determination of the streamwise influence lengths.

Reda and Murphy[14,15] and Law[8] have attempted to develop correlations for shock impingement on a turbulent boundary layer. The experiments performed by these investigators dealt with the relationship between the upstream influence length and the pressure rise across a two-dimensional shock, but did not address the effects of the variation of Mach number. Reda and Murphy relate the upstream influence to the pressure rise across the interaction region, and not to the inviscid pressure rise. Law specifies the upstream influence in terms of the axial location of the separation point. This rules out the use of these relations for the a priori determination of the streamwise influence region. Also, there are questions regarding the two-dimensionality of Reda and Murphy's experiments.[14,15]

Some work has been performed to develop correlations for the streamwise influence regions of an expansion corner flow. Chung[16] and Lu and Chung[17] have considered the flow over an expansion corner and have developed a downstream influence scaling for the turbulent flow past expansion corners. However, the scaling does not address the variation of Reynolds number and hence is limited in its application. Chew[18] has presented experimental results for the shock-wave boundary-layer interaction in the presence of an expansion corner. Narasimha and Sreenivasan[19] have presented results on the relaminarization of expansion corner flows.

The absence of adequate and accurate theoretical, empirical or experimental relations, relating the streamwise influence lengths with the known flow parameters, for a two-dimensional supersonic turbulent flow, was the impetus for the current study. The correlations obtained in this study are validated against experimental and numerical data obtained by other investigators. These correlations can be calculated with ease as they involve only known flow parameters, namely, the freestream Mach number M_∞, freestream Reynolds number per unit length Re, and the magnitude of the inviscid pressure change across the flowfield $\Delta p/p_\infty$. The supersonic turbulent flowfields were computed using the TIPNS algorithm developed by Tannehill et al.[20] The turbulent flow is modeled using the relaxation eddy-viscosity model of Shang and Hankey.[21,22]

Governing Equations

The governing equations are the compressible parabolized Navier–Stokes (PNS) equations, with turbulence closure provided by the relaxation eddy-viscosity model of Shang and Hankey. Upstream effects are accounted for by using multiple streamwise

Received 9 February 2001; revision received 20 July 2003; accepted for publication 25 July 2003.

*Graduate Research Assistant, Department of Aerospace Engineering. Student Member AIAA.

†Manager, Computational Fluid Dynamics Center, and Professor, Department of Aerospace Engineering. Fellow AIAA.

sweeps of the flowfield. The PNS equations, written in a three-dimensional generalized coordinate system (ξ, η, ζ), are[20]

$$\boldsymbol{E}_{\xi} + \boldsymbol{F}_{\eta} + \boldsymbol{G}_{\zeta} = 0 \tag{1}$$

The system of equations is closed by the perfect gas law, and the laminar coefficient of viscosity is calculated using Sutherland's law. A laminar Prandtl number of 0.7 and a turbulent Prandtl number of 0.9 are used in the computations.

In the presence of any disturbance such as an impinging shock in a compressible turbulent flow, the interaction of the flow ahead of, and through the shock, causes the turbulent flow to be influenced by the history of the flow and making the flow essentially nonequilibrium. Therefore, an algebraic turbulence model, which does not incorporate any information about the influence of flow history on the eddy viscosity, would not model the physics of the separated flow accurately and would be unreliable. To overcome this problem in such a manner as to still retain the simplicity of the algebraic models, the relaxation eddy-viscosity model was introduced by Shang and Hankey,[21] mainly as an engineering approximation. This model, which incorporates the effects of the flow history, is based on experimental observations that in a highly accelerated or decelerated turbulent flow the Reynolds shear stress remains nearly frozen at its initial value while being convected along streamlines and then exponentially approaches a new equilibrium state.[21]

In general, it is acknowledged that complex turbulence models, such as two-equation models and direct-numerical simulations (DNS) and large-eddy simulations (LES), capture the details of the shock boundary-layer interactions more accurately than the simple relaxation eddy-viscosity model. However, it was found that the relaxation model performed very well in accurately capturing the start and end of the streamwise interaction regions, which are the focus of the current research. This is demonstrated by the comparison of the present results with experimental and numerical results from other investigators. Thus, this model captures the essential features of the flow physics required for the current study, while keeping the complexity to a bare minimum.

The relaxation eddy-viscosity model consists of a simple algebraic relation for the nonequilibrium turbulent eddy viscosity given by

$$\mu_T = \mu_{T_0} + \left(\mu_{T_{\text{eq}}} - \mu_{T_0}\right)\left[1 - e^{-(\Delta x/\lambda)}\right] \tag{2}$$

where μ_T is the relaxing turbulent eddy viscosity, $\mu_{T_{\text{eq}}}$ is the local equilibrium value of eddy viscosity, and μ_{T_0} is the equilibrium eddy viscosity at a reference location. The distance between a reference station at which relaxation is initiated and the current station is Δx, and the equilibrium values of eddy viscosity μ_{T_0} and $\mu_{T_{\text{eq}}}$ are generated using a standard equilibrium eddy-viscosity model. For the present calculations the Cebeci–Smith model[23] used by Shang and Hankey was replaced by the Baldwin–Lomax model.[23] The Baldwin–Lomax model defines the eddy viscosity soley in terms of the easily calculable quantities like the vorticity, making the model more suitable for the current study, as it is difficult to establish a clear edge for the turbulent boundary layer in shock separated flows.

For all of the computed cases, the reference location was considered to have a fixed value given by Shang and Hankey as

$$x_{\text{relax}} = x/L = 0.9027$$

where L is the distance from the leading edge to the compression ramp/expansion corner location for ramp and corner flows. For the case of a shock impingement, L is the distance from the leading edge to the inviscid shock-impingement point. In the current study λ is given by

$$\lambda = 5\delta_0 \text{ for compression ramp flows}$$

$$\lambda = 2\delta_0 \text{ for expansion corner flows}$$

$$\lambda = 20\delta_0 \text{ for shock impingement flows}$$

where δ_0 is the boundary-layer thickness of the flow at the location immediately upstream of the interaction region. The choice of different values of λ for the flows was based both on comparison with experimental data and on a detailed study of the effects of the variation of λ on the correlations developed.[24,25]

Numerical Algorithm

The PNS equations are well suited for the computation of attached, supersonic viscous flows. However, because the PNS equations are normally solved using a single-sweep space-marching method they are not suitable for the computation of flows with upstream influences. To compute flows with streamwise influence effects, modifications to the PNS algorithm must be made. This led Miller et al.[1] and Tannehill et al.[20] to develop the iterated PNS and the time-iterated PNS (TIPNS) algorithms to compute flows with streamwise influences. In these algorithms multiple streamwise sweeps of the flowfield are made in order to include upstream effects. The PNS equations admit ellipticity in the crossflow plane, and hence any upstream effects occurring in the crossflow plane are automatically computed.

The TIPNS algorithm uses the Steger–Warming flux splitting in the streamwise direction. The $\boldsymbol{E}$ vector is split based on the eigenvalues of $\partial \boldsymbol{E}/\partial \boldsymbol{U}$, so that

$$\boldsymbol{E} = \boldsymbol{E}^{+} + \boldsymbol{E}^{-} = A^{+}\boldsymbol{U} + A^{-}\boldsymbol{U} \tag{3}$$

where A^{+} and A^{-} are the Jacobian matrices based on the positive and negative eigenvalues. The streamwise gradient of $\boldsymbol{E}$ is then discretized using a backward difference for $\partial \boldsymbol{E}^{+}/\partial \xi$ and a forward difference for $\partial \boldsymbol{E}^{-}/\partial \xi$. Details of the TIPNS method are given in Ref. 20.

Correlation Functions

Using dimensional analysis, it can be shown that in a two-dimensional flow the streamwise regions of influence should depend on the following flow parameters, namely, freestream Mach number M_∞, freestream Reynolds number per unit length Re, the magnitude of the overall pressure change $\Delta p/p_\infty$ (or the angle θ causing the pressure change), and the thickness of the undisturbed boundary layer δ_L. The dimensional analysis assumes an adiabatic wall boundary condition. The laminar and turbulent Prandtl numbers and the specific heat ratio are also assumed to be constant.

Dimensional analysis then results in the following forms of the functions for the lengths of the streamwise influence regions:

$$\frac{l_u}{\delta_L} = F\left[Re, \frac{\delta_L}{L}, M_\infty, \frac{\Delta p}{p_\infty}\right] \tag{4}$$

$$\frac{l_d}{\delta_L} = G\left[Re, \frac{\delta_L}{L}, M_\infty, \frac{\Delta p}{p_\infty}\right] \tag{5}$$

The upstream influence length is denoted by l_u and the downstream influence length by l_d. l_u/δ_L is the upstream influence length ratio, and l_d/δ_L is the downstream influence length ratio. The correlations for shock impingement and expansion corner flow have a boundary condition of no influence in the absence of a disturbance to force the functions to follow the physics of the flow, that is,

$$\left(\frac{l_u}{\delta_L} \to 0 \quad \text{and} \quad \frac{l_d}{\delta_L} \to 0\right) \quad \text{as} \quad \frac{\Delta p}{p_\infty} \to 0 \tag{6}$$

The TIPNS algorithm has been demonstrated by Miller et al.[1] and Tannehill et al.[20] to be accurate over the range of flow conditions that are considered in the present study. The accuracy of the turbulent relaxation model in computing turbulent flows is demonstrated later in the current study. Over 100 compression ramp cases, 33 expansion corner cases and 34 shock-impingement cases with differing flow parameters, that is, different combinations of M_∞, Re, and $\Delta p/p_\infty$, were computed using the TIPNS algorithm. Regression analysis using the least-squares approach was used to obtain the exponents of the flow parameters and to develop a final form for the correlations. The exponents for the flow parameters were obtained by cross plots of the flow variables.

To validate the numerically computed data points, experimental data were obtained from Refs. 8–18 and Refs. 21, 22, 26 and 27. The references, including the digital databases, generally provide the experimental data in the form plots of mean flow profiles, wall pressure, and skin-friction data. The start and end of the streamwise influence regions are not always quantified, that is, a numerical value for l_u/δ_L and l_d/δ_L is not given for all experimental data. Therefore, some of the experimental data had to be deduced or extrapolated from the data presented by the authors.

Upstream Correlation Functions

In previous studies the upstream influence length has been determined using either the separation-length criterion or the upstream-pressure-influence criterion. The criterion of separation length is not suitable, as it assumes that only separated flows are being considered, whereas the current study considers both separated and attached flows. The upstream pressure influence criterion used by several experimental investigators is not conducive to numerical analysis. Hence, in the current study the criterion used to obtain the upstream influence length was an engineering criterion rather than a theoretical one. The start of the upstream influence was defined as the x location at which the skin friction of the disturbed solution differed from the value obtained for the undisturbed flow over a flat plate by 1%. While recognizing that this is an ad hoc criterion, it should be noted that it provides an accurate numerical method of identifying the streamwise start of influence. With this criteria the final form of the upstream correlation functions were found to be as follows:

Compression ramps:

$$\frac{l_u}{\delta_L} = 48\frac{\exp\left(0.1\,\theta + M_\infty^{0.3}\right)}{(Re_{\delta_L})^{5/9}} \tag{7}$$

Expansion corners:

$$\frac{l_u}{\delta_L} = 100\left[\frac{(|\Delta p|/p_\infty)^{1/10}}{(M_\infty)^{9/10}(Re_{\delta_L})^{5/9}}\right] \tag{8}$$

Shock impingement:

$$\frac{l_u}{\delta_L} = 273\left[\frac{(\Delta p/p_\infty)^{4/3}}{(M_\infty)^{7/5}(Re_{\delta_L})^{1/3}}\right] \tag{9}$$

where Re_{δ_L} is the Reynolds number based on δ_L. The correlation functions along with the numerical and experimental data are plotted in Figs. 1–3.

For the case of a compression ramp (see Fig. 1), a comparison has been made with the upstream influence length obtained in

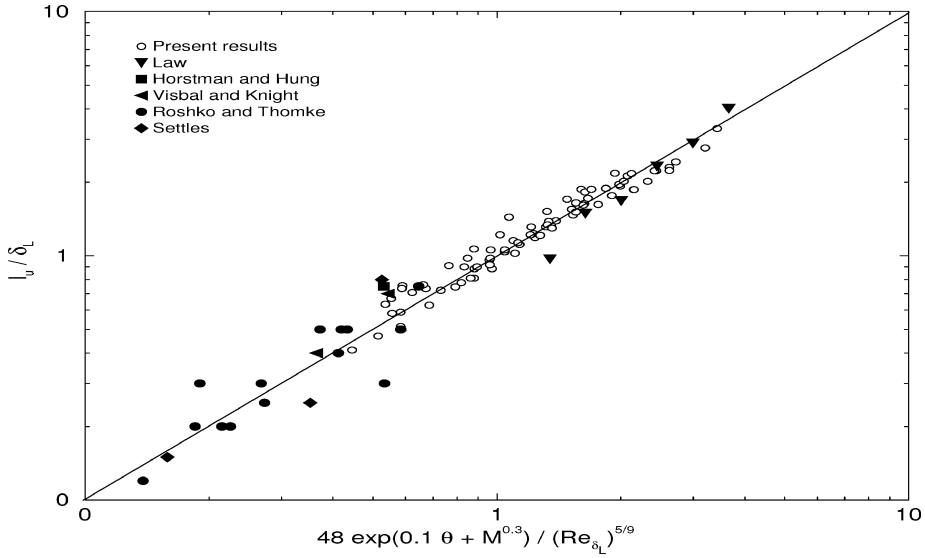

Fig. 1 Upstream correlation function for compression ramps.

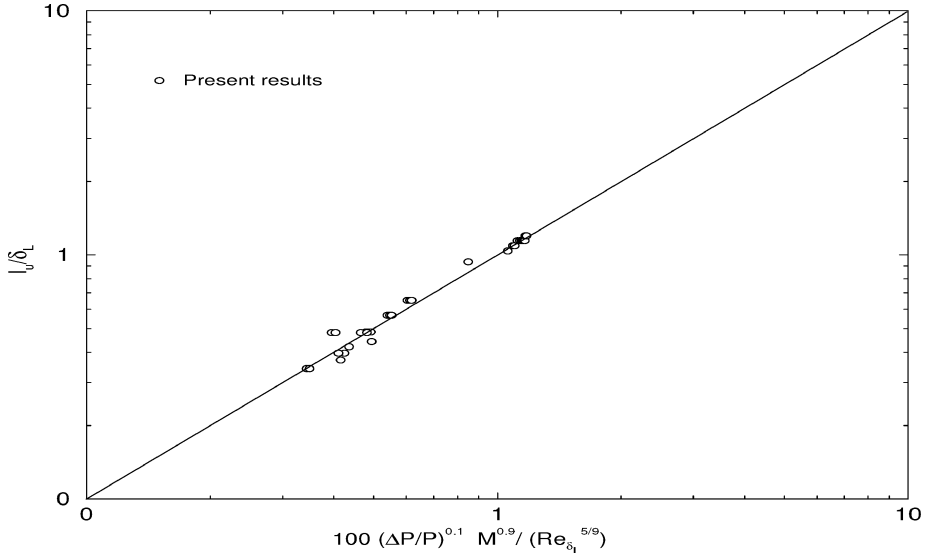

Fig. 2 Upstream correlation function for expansion corners.

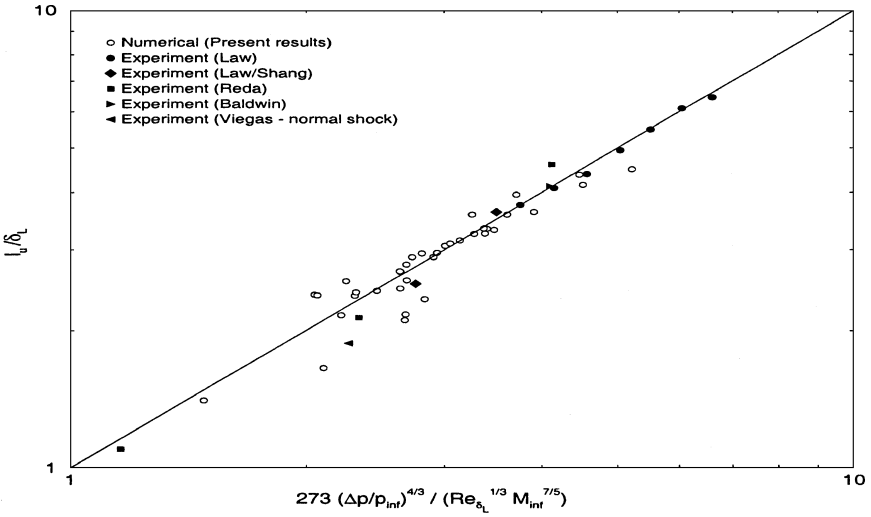

Fig. 3 Upstream correlation function for shock impingement.

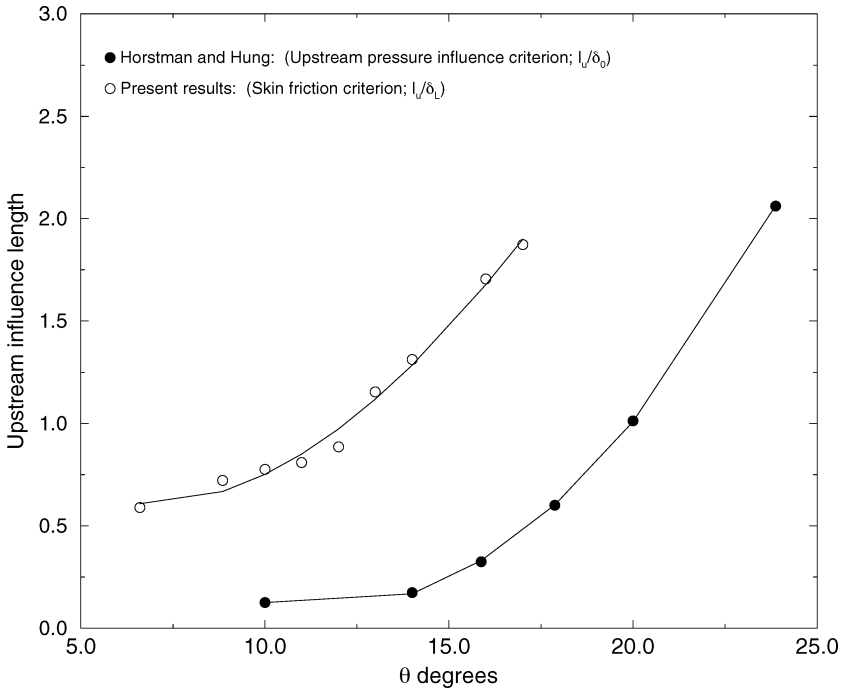

Fig. 4 Comparison of criteria for upstream influence length for a compression ramp.

various experiments.[4–11] The flow parameters in these experiments are within the valid range of the developed correlation function. From Fig. 1 it can be seen that the difference between the predicted and actual value of l_u/δ_L is significantly less than one boundary-layer thickness δ_L for all of the data, with a maximum difference of 0.32 δ_L. An exponential function was found to give the best fit for the data in the range considered for the case of a compression ramp, and hence the boundary condition of Eq. (6) was relaxed. An exponential scaling of the upstream influence was also presented by Settles et al.,[13] who developed the scaling of the upstream pressure influence parameter based on a surface pressure criterion. A comparison of the upstream influence length prediction using the experimental upstream pressure influence criterion results[11] and the skin-friction criterion used in the current study is shown in Fig. 4. The results are plotted for $Re_{\delta_0} \sim 1.3 \times 10^6$. The trend of the data is similar for both the criteria, with the present skin-friction criterion predicting a larger upstream influence length.

For the case of an expansion corner (see Fig. 2), the numerical data obtained for the upstream influence length scaled well with the simple correlation developed. According to Narasimha and Sreenivasan,[19] the interaction region for an expansion corner flow is insensitive to the corner deflection angle for low supersonic flows. This was corroborated in the current study where it was found that the upstream influence length l_u is independent of the corner deflection angle for fixed values of Mach and Reynolds numbers. The experimental results from Refs. 16–18 did not include skin-friction data and hence could not be used for comparison with the upstream correlation function.

For shock-impingement flows (see Fig. 3) comparisons have been made with the experimental data from Refs. 8, 14, 22, 26 and 27. Further details regarding the development of the upstream correlation function for shock-impingement flows are given in Refs. 24 and 25.

From Figs. 1–3 it can be seen that the correlation functions accurately predict the extent of upstream influence for all of the flowfields considered. It can be seen that the difference between the predicted and actual values of l_u/δ_L is significantly less than one boundary-layer thickness δ_L.

Downstream Correlation Functions

The criterion used to obtain l_d was also based on an engineering criterion. For compression ramps and shock-impingement flowfields

the end of the downstream influence was defined as the x location at which the value of the pressure from the numerical solution differed from the asymptotic value of the numerical solution by 1%. In the case of expansion corners, the end of the downstream influence was defined as the x location at which the value of the pressure from the numerical solution differed from the asymptotic value of the numerical solution by 5%.

The asymptote of the numerical solution was chosen instead of the inviscid asymptote in order to be consistent with the numerically computed solution. As the computed asymptote matches the inviscid asymptote, this was considered to be acceptable. The pressure criteria was employed to determine the downstream end of influence, as opposed to the skin-friction criteria because it was observed that downstream rise of skin friction is sensitive to the particular turbulence model employed and the parameters used for closure. This can also be observed in the literature[23,26] when comparisons of different turbulence models are made. This made the choice of a pressure criteria more prudent, as the manner in which the pressure rises/drops to the inviscid asymptote is nearly independent of the relaxation parameters and turbulence models used. This provides an adequate method of identifying the streamwise end of influence.

Following the same method used for the upstream influence correlations, the downstream correlation functions were found to be as follows:

Compression ramps:

$$\frac{l_d}{\delta_L} = \frac{0.5\,\theta\,(M_\infty)^{10/3}}{(Re_{\delta_L})^{1/3}} \tag{10}$$

Expansion corners:

$$\frac{l_d}{\delta_L} = 2.2\left(\frac{|\Delta p|}{p_\infty}\right)^{\frac{3}{2}} M_\infty^{\frac{9}{5}}\left(1 + \frac{1}{Re_{\delta_L}^{1/10}}\right) \tag{11}$$

Shock impingement:

$$\frac{l_d}{\delta_L} = 3.3\left[\frac{\left[\frac{3}{2}(\Delta p/p_\infty)\right]\left(Re_{\delta_L}\right)^{2/15}}{\left(M_\infty^{4/3}+1\right)}\right]^{0.75} \tag{12}$$

The downstream correlation functions are plotted in Figs. 5–7. Comparison with accurate experimental data for all of the downstream correlation functions could not be made, as the existing experimental data would have to be extrapolated to match the present criterion. However, to examine the trends of the correlations some of the experimental data from Ref. 4 have been extrapolated for the compression ramp flowfield and plotted in Fig. 5. It can be seen that the downstream correlation scales well with the extrapolated experimental data.

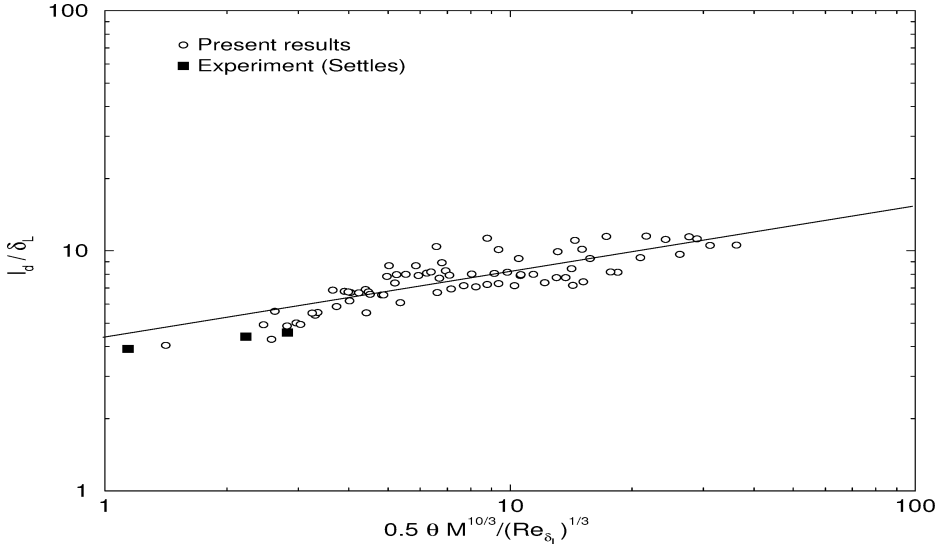

Fig. 5 Downstream correlation function for compression ramps.

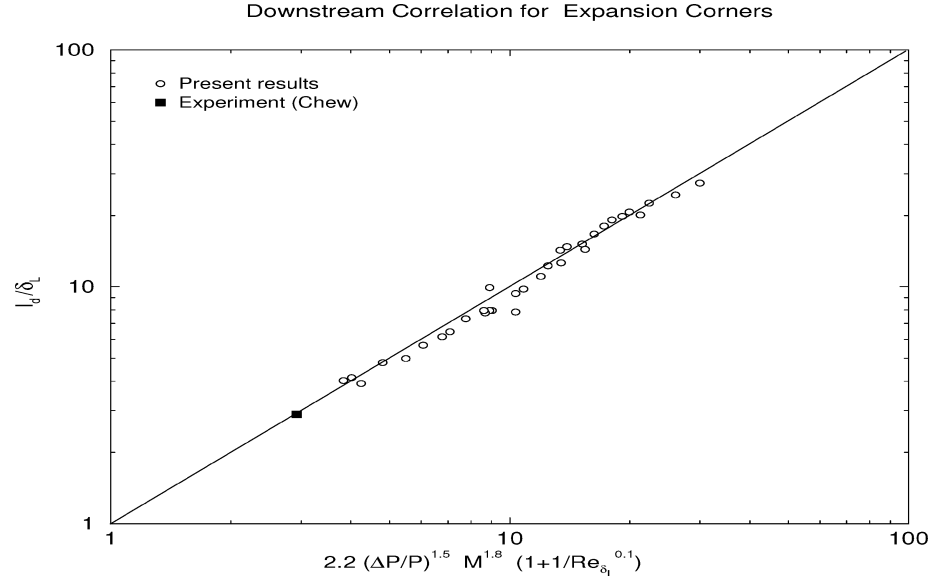

Fig. 6 Downstream correlation function for expansion corners.

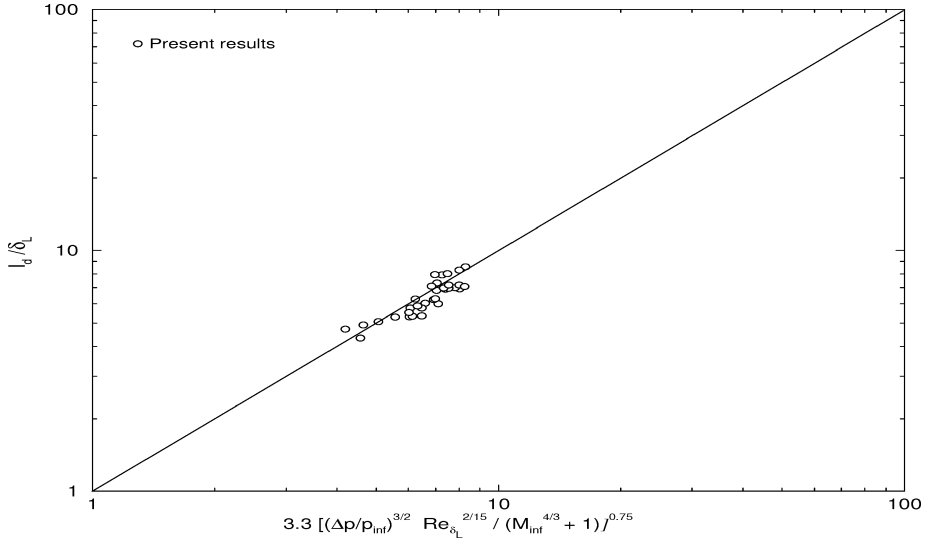

Fig. 7 Downstream correlation function for shock impingement.

For the case of the expansion corner (see Fig. 6), the numerical data obtained for the downstream influence length scaled well with the simple correlation developed. A comparison of the downstream correlation function with the experimental data of Chew[18] is made. According to Chung,[16] the downstream influence length of a expansion corner can be scaled with the hypersonic similarity parameter K. This was corroborated in the current study, where it was found that the downstream influence length l_d scaled to the hypersonic similarity parameter K, with a distinct slope for each Mach number. Additional details are provided in Ref. 28.

The downstream correlation function for a shock-impingement case is presented in Fig. 7. Further details regarding the development of the downstream correlation function for shock-impingement flows are provided in Refs. 24 and 25.

Range of Validity of Correlations

Both the upstream and downstream correlation functions have been found to be accurate over a wide range, as can been seen by the accuracy of these functions in scaling the experimental data points. The ranges of validity for the various flowfields are as follows:

Compression ramps:

$$2.5 \le M_\infty \le 5.0$$

$$3.32 \times 10^6/\text{m} \le Re \le 1.11 \times 10^8/\text{m}$$

$$0.5 \le \Delta p/p_\infty \le 2.68$$

Expansion corners:

$$2.5 \le M_\infty \le 4.5$$

$$3.3 \times 10^6/\text{m} \le Re \le 3.3 \times 10^7/\text{m}$$

$$0.328 \le |\Delta p|/p_\infty \le 0.895$$

Shock impingement:

$$1.4 \le M_\infty \le 5.0$$

$$1.0 \times 10^6/\text{m} \le Re \le 1.0 \times 10^8/\text{m}$$

$$1.0 \le \Delta p/p_\infty \le 5.0$$

The correlation functions that have been presented so far have been developed without any safety factor σ. For regions that have massive separation and also to take into account the vagaries of the present turbulence model, a safety factor of 10% is recommended for both the upstream and downstream correlation functions that have been developed.

The value of the compressible turbulent boundary-layer thickness δ_L required for the present correlations can be readily computed using a basic turbulent flow code. Alternatively, δ_L can be computed using an approximate empirical formula that was developed previously.[24] However, the values of δ_L used in the current study are the actual computed values obtained during calculations.

An interesting byproduct of the development of the upstream correlation function is that user specification of the turbulence closure parameter x_{relax} can be avoided. The upstream correlation function F predicts the streamwise start of upstream influence and is consequently equivalent to the streamwise start of relaxation represented by the parameter x_{relax}. Hence, the streamwise start of relaxation x_{relax} can be calculated a priori as

$$x_{\text{relax}} = F\delta_L$$

where δ_L is the undisturbed boundary-layer thickness at L. This equivalence implies that the arbitrary closure parameter x_{relax} of the relaxation model can be quantified using an empirical relation, namely, F, leaving just one closure parameter λ as user specified.

Test Cases

The test cases presented here are four of the over 167 numerically computed compression ramp, expansion corner, and shock-impingement flowfields that were used to obtain the correlation functions. The compression ramp test cases presented correspond to the experiments performed by Law,[8] Settles and Dadson,[4] and Zheltovodov.[2] The expansion corner test case corresponds to the experiment of Chung.[16] The shock-impingement test case corresponds to the experiment performed by Law.[8] Several other comparisons with experimental data are also presented in Refs. 24 and 28. The TIPNS algorithm with the turbulence relaxation model was used to compute the solutions. This algorithm requires the region where the solution is iterated to be specified beforehand. The rest of the flow is computed by a single-sweep space marching technique.[1,20] This specification was done in such a way that the iterated region encompassed the streamwise influence region. To ensure the independence of the computed solution on the specification of the region of iteration, computations were made varying the extent of the iteration region, and no practical difference was found between the solutions. Comparisons were also made with the OVERFLOW Navier–Stokes code[29] and the Navier–Stokes calculations of Shang and Hankey.[21,22] For the compression ramp comparison has also been made with the LES results of Urbin and Knight.[30] The computed solutions were subject to a series of grid-refinement studies, and the results are grid independent.

Case 1: Compression Ramp (θ = 15.0 deg)

The flow parameters for this adiabatic wall compression ramp test case, which correspond to the experiments of Law,[8] are

$$M_\infty = 2.96, \qquad Re = 3.94 \times 10^7/\text{m}, \qquad T_\infty = 98.91$$

The grid-independent results for pressure and skin friction are plotted in Figs. 8 and 9. The present results are compared with Navier–Stokes results and also with the experimental results of Law. It can be seen that the values of the computed pressure (see Fig. 8) using the present relaxation model are in good agreement with the experimental data points obtained by Law throughout the flowfield. A small difference exists in the region of the separated flow, but as the current study is concerned with only the streamwise extent of influence, and not in capturing all of the details of the turbulent flow, this deviation was not considered significant. For this test case it was found that using a smaller value for the turbulence closure parameter λ results in better agreement with the experimental pressure data. This is demonstrated in Fig. 8. A value of $\lambda = 2.0\delta_0$ was found to give the best agreement for the pressure data. As a skin-friction criterion is used to predict the upstream influence length, the effect of λ variation on the wall pressure was not considered to be very important.

The skin-friction results given in Fig. 9 are in good agreement with the numerical results from the OVERFLOW Navier–Stokes code in the region leading to separation and in the separated region of the flow. From the figure it is seen that the variation of λ does not have a significant effect on the upstream influence region. The skin-friction plot reveals some differences in the downstream region of flow, after reattachment. However, as the criteria for the end of downstream influence was based on the values of wall pressure, this difference is not considered to be important, as it concerns the details of the turbulent flow and not the extent of influence of the shock separated flow.

To ensure that the developed correlations did not depend on the relaxation model closure parameters x_{relax} and λ, a detailed study was carried out for a wide range of x_{relax} and λ values. It was determined that variation of x_{relax} and λ had no significant effect on predicting the start or the end of the streamwise influence regions. Details of the study are presented in Ref. 25.

Case 2: Compression Ramp (θ = 8.0 deg)

For this test case comparison was made with two sets of experimental data, that is, Settles and Dodson[4] and Zheltovodov.[3] The flow parameters for the Settles and Dodson[4] adiabatic-wall compression ramp case are

$$M_\infty = 2.87, \qquad Re = 6.3 \times 10^7/\text{m}, \qquad (T_{\text{stag}})_\infty = 280$$

The results for wall pressure are presented in Fig. 10. During the computations, the computed boundary-layer thickness was matched to the experimental value of $\delta_0 = 2.6$ cm given in Ref. 4. The

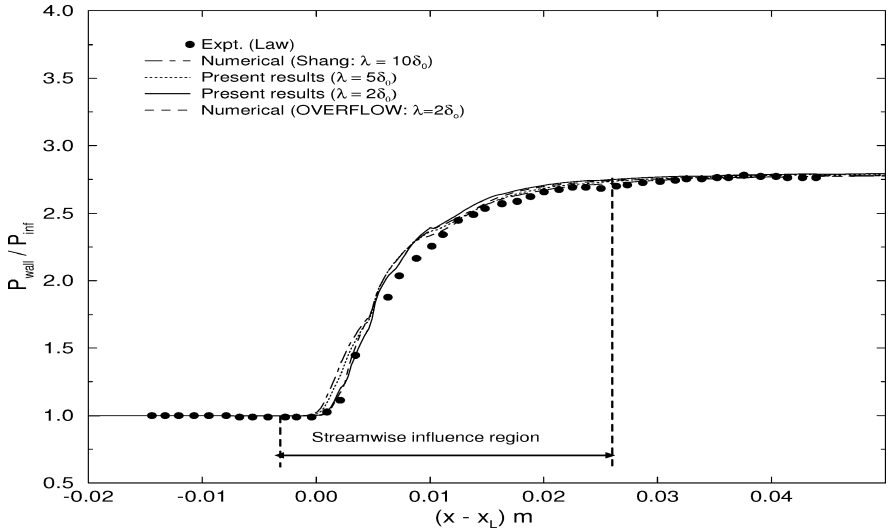

Fig. 8 Wall-pressure results for compression ramp case (θ = 15.0 deg).

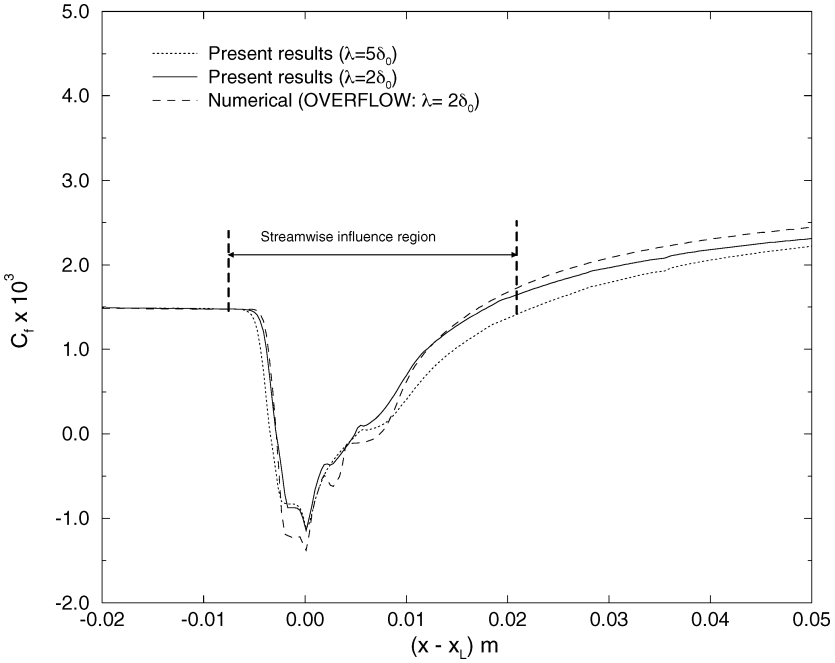

Fig. 9 Skin-friction results for compression ramp case (θ = 15.0 deg).

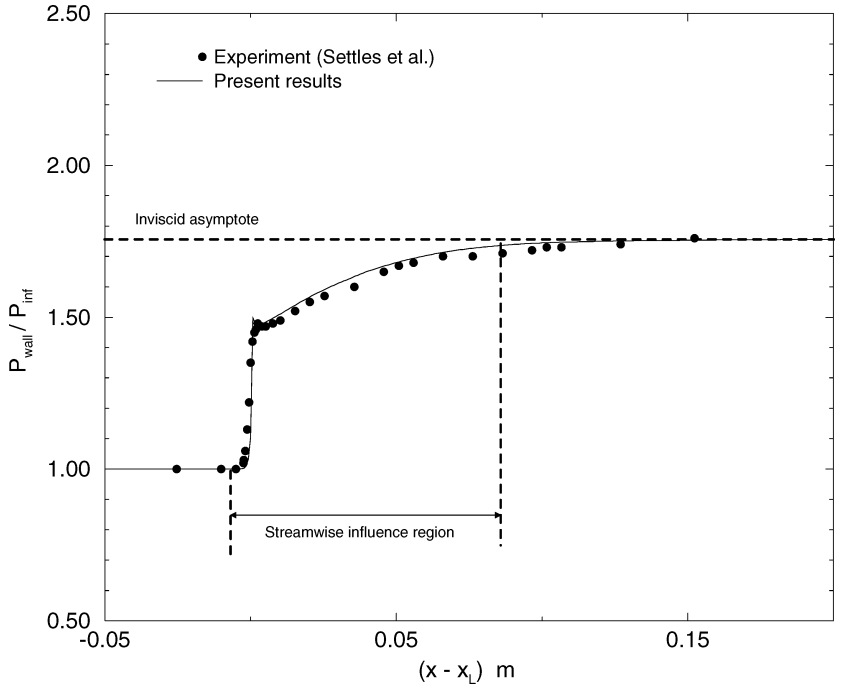

Fig. 10 Wall-pressure results for compression ramp case (θ = 8.0 deg).

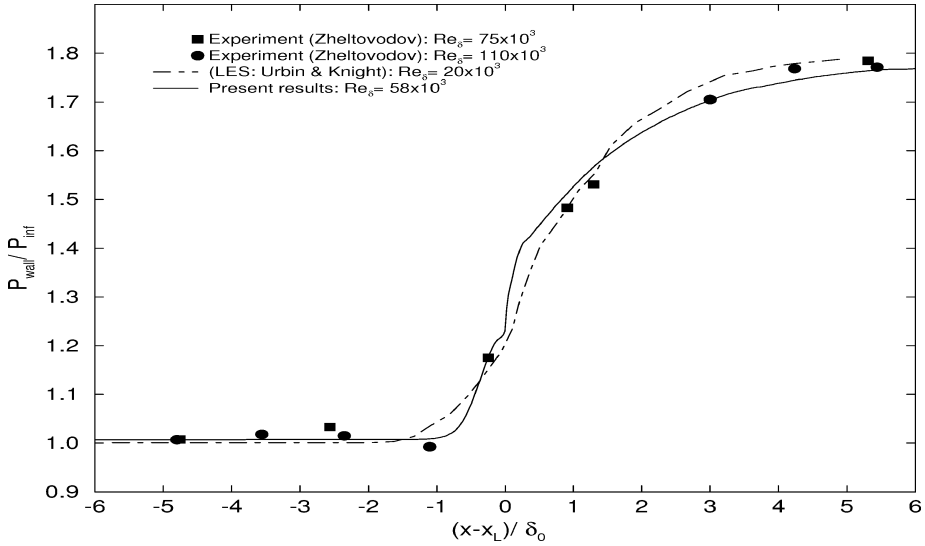

Fig. 11 Wall-pressure results for compression ramp case (θ = 8.0 deg).

computed pressure plot can be seen to be in good agreement with the experimental data.

The flow parameters for the Zheltovodov[3] adiabatic-wall compression ramp case are

$$M_\infty = 2.95, \qquad Re_{\delta_0} = 75 \times 10^3$$

The results for wall pressure are presented in Fig. 11, along with experimental data and the LES results from Ref. 30. Again, a reasonable agreement is seen with both the experimental and LES results. Additional comparisons with experimental data and numerical data for compression ramps are presented in Ref. 28.

Case 3: Shock Impingement (θ = 25.8 deg)

The flow parameters for this adiabatic-wall shock-impingement test case correspond to the experiment of Law[8] and are given by

$$M_\infty = 2.96, \qquad Re = 3.94 \times 10^7/\text{m}, \qquad T_\infty = 89.82$$

and the inviscid pressure rise is

$$\Delta p/p_\infty = 1.949$$

The results are presented in Figs. 12 and 13. The present pressure results (see Fig. 12) are in good agreement with the numerical results of Shang and Hankey, the OVERFLOW code, and with the experimental results of Law. The skin-friction plot (see Fig. 13) reveals some differences in the downstream region of flow, after reattachment. This difference can also be noticed in comparisons with the OVERFLOW code and is also evident in the literature,[26] when different turbulence models are used to model the same flow, with every model revealing differing details in the downstream region. However, the pressure plot (see Fig. 12) indicates that the computed values for pressure for all of the solutions are nearly identical in the reattachment region. As the criteria for the end of downstream influence was based on the values of pressure, this possible source for error was not considered to be important, as it concerns the details of the turbulent flow and not the extent of influence of the shock-separated flow. Additional comparisons with experimental data and numerical data for shock-impingement flows are presented in Ref. 24.

Case 4: Expansion Corner (θ = −10.0 deg)

The flow parameters for this adiabatic-wall expansion corner case correspond to the experiment of Chung[16] and are given by

$$M_\infty = 1.28, \qquad Re = 2.0 \times 10^7/\text{m}, \qquad T_\infty = 98.91$$

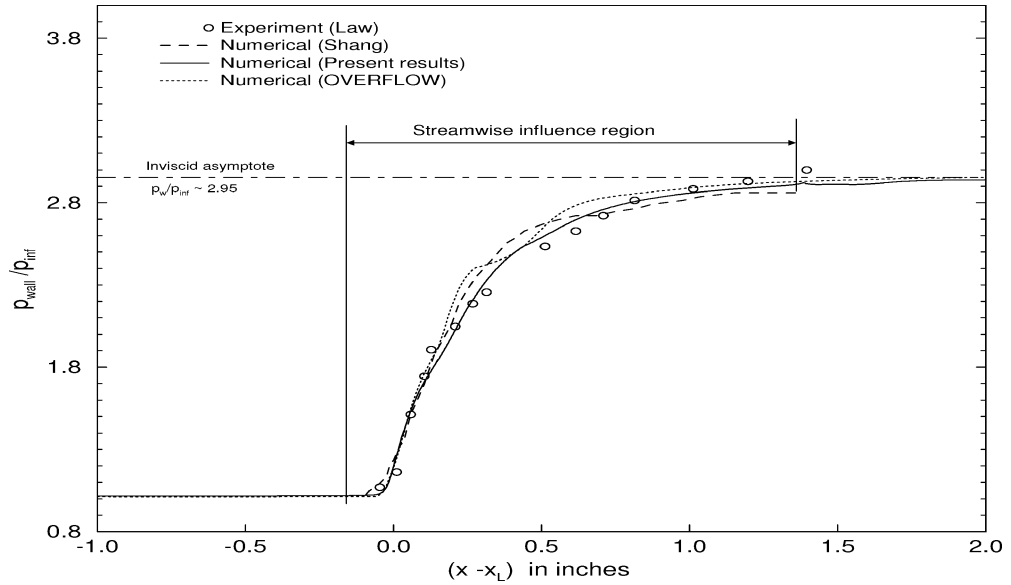

Fig. 12 Wall-pressure results for a shock impingement angle θ = 25.8 deg.

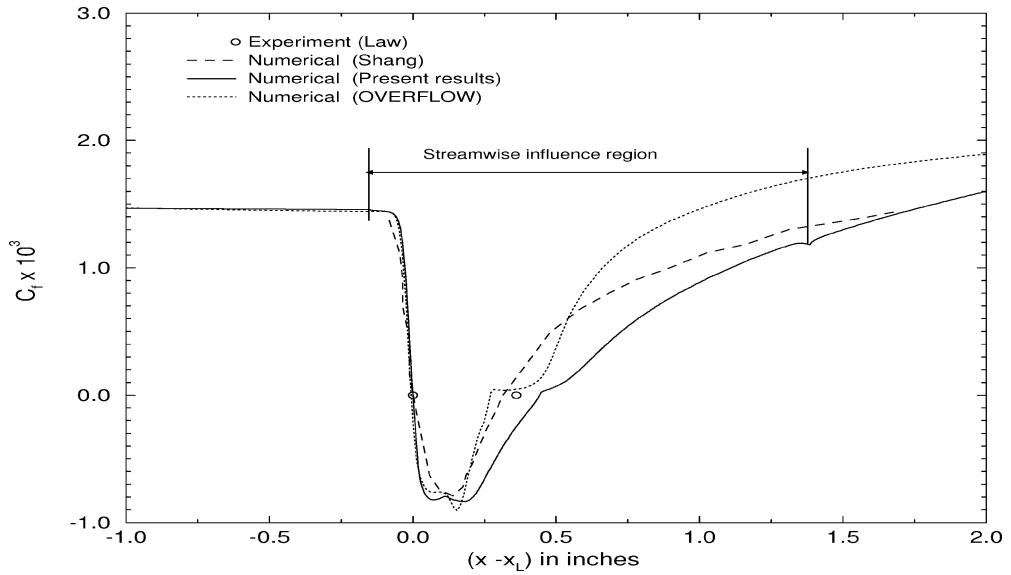

Fig. 13 Skin-friction results for a shock-impingement angle θ = 25.8 deg.

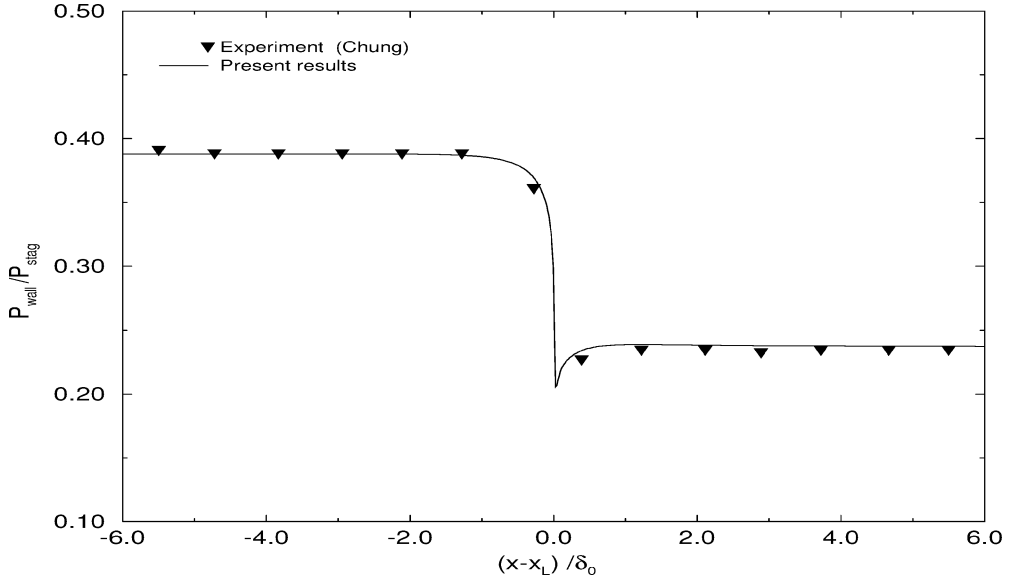

Fig. 14 Wall-pressure results for expansion corner case (θ = −10.0 deg).

and the pressure drop is

$$\Delta p/p_\infty = 0.389$$

The grid-independent results for pressure are presented in Fig. 14. It can be seen that there is good agreement between the present results and the experimental data of Chung[16] throughout the flowfield. However, the flow parameters of this experimental case are not in the valid range of the correlation functions developed for expansion corners. This case was used only to validate the accuracy of the TIPNS algorithm in computing expansion corner flowfields.

Conclusions

In conclusion, correlation functions that depend entirely on known flow variables have been developed to predict the extent of the streamwise influence regions in supersonic turbulent flows. The flowfields considered were compression ramps, expansion corners, and shock-impingement flowfields. The correlations have been applied to test cases, and the computed results were found to be in good agreement with experimental results. The accuracy of these functions in predicting both the upstream and downstream influence regions, for a wide range of data, has been demonstrated. With the current study the streamwise influence regions over a supersonic aircraft geometry can be predicted a priori, facilitating easy and efficient calculation of the flowfield.

References

[1]Miller, J. H., Tannehill, J. C., and Lawrence, S. L., "PNS Algorithm for Solving Supersonic Flows with Upstream Influences," *AIAA Journal*, Vol. 38, No. 10, 2000, pp. 1837–1845.

[2]Zheltovodov, A. A., "Shock Waves/Turbulent Boundary-Layer Interactions—Fundamental Studies and Applications," AIAA Paper 96-1977, June 1996.

[3]Knight, D., and Yan, H., "RTO WG 10: CFD Validation for Shock Wave Turbulent Boundary Layer Interactions," AIAA Paper 2002-0437, Jan. 2002.

[4]Settles, G. S., and Dodson, L. J., "Hypersonic Shock/Boundary-Layer Interaction Database," NASA-CR 177577, April 1991.

[5]Settles, G. S., and Dodson, L. J., "Hypersonic Shock/Boundary-Layer Interaction Database: New and Corrected Data," NASA-CR 177638, April 1994.

[6]Delery, J., and Marvin, J. G., "Shock Wave Boundary-Layer Interactions," AGARDograph AG-280, Advisory Group for Aerospace Research and Development, Neuilly-sur-Seine, France, Feb. 1986.

[7]Hankey, W. L., and Holden, M. S., "Two-Dimensional Shock Wave-Boundary Layer Interactions in High Speed Flows," AGARDograph AG-203, Advisory Group for Aerospace Research and Development, Neuilly-sur-Seine, France, June 1975.

[8]Law, H. C., "Supersonic Shock Wave Turbulent Boundary-Layer Interactions," *AIAA Journal*, Vol. 14, No. 6, 1976, pp. 730–734.

[9]Roshko, A., and Thomke, G. J., "Supersonic, Turbulent Boundary-Layer Interaction with a Compression Corner at Very High Reynolds Number," *Proceedings of the Symposium on Viscous Interaction Phenomena in Supersonic and Hypersonic Flow*, USAF Aerospace Research Labs., Wright–Patterson AFB, Univ. of Dayton Press, Dayton, OH, 1969, pp. 109–138.

[10]Visbal, M., and Knight, D., "The Baldwin-Lomax Turbulence Model for Two-Dimensional Shock-Wave/Boundary-Layer Interactions," *AIAA Journal*, Vol. 22, No. 7, 1984, pp. 921–928.

[11]Horstman, H. C., and Hung, C. M., "Reynolds Number Effects on Shock-Wave Turbulent Boundary-Layer Interactions—A Comparison of Numerical and Experimental Results," AIAA Paper 77-42, Jan. 1977.

[12]Settles, G. S., and Bogdonoff, S. M., "Scaling of Two-and Three-Dimensional Shock/Turbulent Boundary-layer Interactions at Compression Corners," *AIAA Journal*, Vol. 20, No. 6, 1982, pp. 782–789.

[13]Settles, G. S., Bogdonoff, S. M., and Vas, I. E., "Incipient Separation of a Supersonic Turbulent Boundary Layer at High Reynolds Numbers," *AIAA Journal*, Vol. 14, No. 1, 1976, pp. 50–56.

[14]Reda, D. C., and Murphy, J. D., "Shock Wave/Turbulent Boundary-Layer Interactions in Rectangular Channels," *AIAA Journal*, Vol. 11, No. 2, 1973, pp. 139, 140.

[15]Reda, D. C., and Murphy, J. D., "Sidewall Boundary-Layer Influence on Shock Wave/Turbulent Boundary-Layer Interactions," *AIAA Journal*, Vol. 11, No. 10, 1973, pp. 1367, 1368.

[16]Chung, K., "Interaction Region of Turbulent Expansion-Corner Flow," *AIAA Journal*, Vol. 36, No. 6, 1998, pp. 1115, 1116.

[17]Lu, F. K., and Chung, K. M., "Downstream Influence Scaling of Turbulent Flow Past Expansion Corners," *AIAA Journal*, Vol. 30, No. 12, 1992, pp. 2976, 2977.

[18]Chew, Y. T., "Shockwave and Boundary Layer Interaction in the Presence of an Expansion Corner," *Aeronautical Quarterly*, Vol. **XXX**, Aug. 1979, pp. 506–527.

[19]Narasimha, R., and Sreenivasan, K. R., "Relaminarization of Fluid Flows," *Advances in Applied Mechanics*, edited by Chia-Shan Yih, Vol. 19, Academic Press, New York, NY, 1979, pp. 221–309.

[20]Tannehill, J. C., Miller, J. H., and Lawrence, S. L., "Development of an Iterative PNS Code for Separated Flows," AIAA Paper 99-3361, June 1999.

[21]Shang, J. S., and Hankey, W. L., "Numerical Solution of The Navier–Stokes Equations for Supersonic Turbulent Flow over a Compression Ramp," AIAA Paper 75-3, Jan. 1975.

[22]Shang, J. S., and Hankey, W. L., "Numerical Simulation of Shock Wave-Turbulent Boundary-Layer Interaction," *AIAA Journal*, Vol. 14, No. 10, 1976, pp. 1451–1457.

[23]Wilcox, D. C., *Turbulence Modeling for CFD*, 2nd ed., DCW Industries, La Cañada, CA, 2000.

[24]Ramesh, M. D., Tannehill, J. C., and Miller, J. H., "Correlations to Predict the Streamwise Influence Regions of Two-Dimensional Turbulent Shock Separated Flows," AIAA Paper 2000-0932, Jan. 2000.

[25]Ramesh, M. D., "Correlations to Predict the Streamwise Influence Regions of Two-Dimensional Turbulent Shock Separated Flows," M.S. Thesis, Dept. of Aerospace Engineering, Iowa State Univ., Ames, IA, Feb. 1999.

[26]Viegas, J. R., and Horstman, C. C., "Comparison of Multi-Equation Turbulence Models for Several Shock Separated Boundary-Layer Interaction Flows," AIAA Paper 78-1165, July 1978.

[27]Baldwin, B. S., and MacCormack, K. W. "Modifications of the Law of the Wall and Algebraic Turbulence Modeling for Separated Boundary Layers," AIAA Paper 76-350, July 1976.

[28]Ramesh, M. D., and Tannehill, J. C., "Correlations to Predict the Streamwise Influence Regions of 2-D Turbulent Flows," AIAA Paper 2001-0884, Jan. 2001.

[29]Buning, P. G., Jespersen, D. C., and Pulliam, T. H., OVERFLOW Manual, Ver. 1.7v, NASA Ames Research Center, Moffett Field, California, June 1997.

[30]Urbin, G., and Knight, D.,"Compressible Large Eddy Simulation Using Unstructured Grid: Supersonic Turbulent Boundary Layer and Compression Corner," AIAA Paper 1999-0427, Jan. 1999.